

SHARDS OF BROKEN SYMMETRY: TOPOLOGICAL DEFECTS AS TRACES OF THE PHASE TRANSITION DYNAMICS*

W.H. ZUREK, L.M.A. BETTENCOURT, J. DZIARMAGA

Theoretical Division, Los Alamos National Laboratory
Los Alamos NM 87545, USA

AND N.D. ANTUNES

Dépt. de Physique Théorique, Université de Genève
24 quai E. Ansermet, CH 1211, Genève 4, Switzerland

(Received October 6, 2000)

We discuss the origin of topological defects in phase transitions and analyze their role as a “diagnostic tool” in the study of the non-equilibrium dynamics of symmetry breaking. Homogeneous second order phase transitions are the focus of our attention, but the same paradigm is applied to the cross-over and inhomogeneous transitions. The discrepancy between the experimental results in ^3He and ^4He is discussed in the light of recent numerical studies. The possible role of the Ginzburg regime in determining the vortex line density for the case of a quench in ^4He is raised and tentatively dismissed. The difference in the anticipated origin of the dominant signal in the two (^3He and ^4He) cases is pointed out and the resulting consequences for the subsequent decay of vorticity are noted. The possibility of a significant discrepancy between the effective field theory and (quantum) kinetic theory descriptions of the order parameter is briefly touched upon, using atomic Bose–Einstein condensates as an example.

PACS numbers: 05.70.Fh

1. Introduction

The theory of the creation of topological defects appeals to models of critical dynamics and to our understanding of the processes which occur when phase transitions take place. Consequently, topological defects can be used as “symptoms”, macroscopic manifestations of underlying physical processes, which in turn can help diagnose the nature of critical dynamics.

* Presented at the XL Cracow School of Theoretical Physics, Zakopane, Poland, June 3–11, 2000. The paper is based on the material published in Ref. [41].

For first order phase transitions there is little doubt that nucleation — a process understood for over half a century — is an essentially accurate, universal yet simple model. A similarly simple model of the dynamics of second order phase transitions was proposed much more recently [1–3]. One of its implications is the ability to predict the size of the ordered patches of the new lower symmetry phase, right from its inception. This allows one to calculate the initial density of topological defects through the estimate put forward in the seminal paper by Kibble [4,5]. It may also lead to a revision of the scenarios for baryogenesis and chiral symmetry restoration [6, 7], as well as other related phenomena (such as the A–B ^3He transition, see [8,9]). Some of the predictions based on the new paradigm have been successfully tested and refined in numerical experiments [10–14]. More importantly the prediction of copious vortex production in superfluid phase transitions has been experimentally verified in ^3He by two very different strategies in two distinct parameter regimes [15,16]. The situation in ^4He [17] and the initial indications from high temperature superconductors [18] are, however, at best inconclusive. Indeed there are still differences concerning analytic estimates of the initial density of defects in the underdamped case [19,20], even in 1D. The aim of this paper is two-fold: We shall start with a brief summary of the paradigm on which the emerging understanding of second order phase transitions is based. We shall then explore its extrapolations and investigate the experimental, numerical and analytic evidence for and against this mechanism, in various settings. This paper is not really an introductory survey to the extent to which our lectures were. We have decided that the existing literature (including the reviews of Zurek [21] and Eltsov, Krusius and Volovik [22] as well as the other papers mentioned above and below) already serves this purpose. Rather we aim to perform a “reconnaissance by force” of what is likely to be the most interesting “proving grounds” for the ideas summarized briefly in the following section.

2. Critical dynamics and defect formation

Second order transitions fall into universality classes which are characterized by the behavior of the healing length ξ and the relaxation time τ (among other quantities) as a function of the relative temperature

$$\varepsilon(T) = \frac{T - T_c}{T_c}. \quad (1)$$

Thus, $\tau \sim |\varepsilon|^{-\nu z}$ and $\xi \sim |\varepsilon|^{-\nu}$ diverge in the vicinity of $\varepsilon = 0$, where ν and z are universal critical exponents. A very specific model which represents a large class of second order phase transitions is the so-called Landau–Ginzburg theory. There, the dynamics of the order parameter is thought to

effectively obey a Langevin equation of the form:

$$\ddot{\varphi} + \eta\dot{\varphi} - c^2\nabla^2\varphi + \frac{1}{2} [\lambda\varphi^3 + m^2\phi] = \mathcal{O}(t, x). \tag{2}$$

Above, η characterizes the viscosity in the system, while c, λ are constant coefficients. The mass term m^2 can depend explicitly on time. Moreover, the correlation function for the noise

$$\langle \mathcal{O}(t, x)\mathcal{O}(t', x') \rangle = 2\eta\Theta\delta(x - x')\delta(t - t'), \tag{3}$$

includes the temperature parameter Θ , which can vary. The change of m^2 , *e.g.* $m^2 = m_0^2\varepsilon(t)$ or of Θ or both, may precipitate the phase transition.

We shall assume that in the vicinity of the critical temperature $\varepsilon(t)$ obeys a simple relation

$$\varepsilon(t) = \frac{t}{\tau_Q}. \tag{4}$$

In that case the dynamics of the order parameter can be approximately divided into the adiabatic and impulse regimes [2, 3], with the boundary which occurs at time \hat{t} when the relaxation time of the order parameter equals the characteristic time on which $\varepsilon(t)$ changes:

$$\tau(\varepsilon(\hat{t})) = \frac{\varepsilon(\hat{t})}{\dot{\varepsilon}(\hat{t})} = \hat{t}. \tag{5}$$

The timescale on which the order parameter will react to changes of $\varepsilon(t)$ depends on whether $\dot{\varphi}$ or $\ddot{\varphi}$ dominates. For the Landau–Ginzburg theory, in the two cases

$$\tau_{\dot{\varphi}} = \frac{\eta\tau_0^2}{|\varepsilon|}, \quad \tau_{\ddot{\varphi}} = \frac{\eta\tau_0}{|\varepsilon|^2}, \tag{6}$$

respectively, where $\tau_0 = 1/m_0$, and m_0 is the mass term in Eq. (2), evaluated for $T = 0$ (*i.e.* for $\varepsilon = -1$).

Using $\varepsilon(t) = t/\tau_Q$, we can now solve for \hat{t} , to obtain:

$$\hat{t}_{\dot{\varphi}} = \pm\tau_0\sqrt{\eta\tau_Q}, \quad \hat{t}_{\ddot{\varphi}} = \pm\tau_0^{2/3}\tau_Q^{1/3}. \tag{7}$$

To estimate the scale of the domains which could have become uniform through dynamics in the adiabatic regime, we should need:

$$\hat{\varepsilon}_{\dot{\varphi}} = \pm\sqrt{\frac{\eta\tau_0^2}{\tau_Q}}; \quad \hat{\varepsilon}_{\ddot{\varphi}} = \pm\left(\frac{\eta\tau_0^2}{\tau_Q}\right)^{2/3}. \tag{8}$$

The characteristic scale is then given by $\hat{\xi} = \xi_0 / \sqrt{|\hat{\varepsilon}|}$, which yields:

$$\hat{\xi}_{\dot{\varphi}} = \xi_0 \left(\frac{\tau_Q^2}{\eta\tau_0^2} \right)^{1/4} ; \quad \hat{\xi}_{\ddot{\varphi}} = \xi_0 \left(\frac{\tau_Q}{\tau_0} \right)^{1/3} . \quad (9)$$

The initial density of defects can now be estimated using an argument due to Kibble [4], which will imply a $\hat{\xi}$ -sized unit of defect per $\hat{\xi}$ sized volume, *i.e.* $n \sim 1/\hat{\xi}^2$ for vortex strings in two spatial dimensions.

The above calculation is based on the assumption that the order parameter approximates its equilibrium configuration until $-\hat{t}$, at which point it ceases to evolve dynamically (although noise and damping continue unabated). The dynamical evolution restarts at $+\hat{t}$, below the critical point, but by then it may be too late to undo non-trivial topological arrangements of φ inherited from above T_c .

This same paradigm decides when the overdamped or underdamped estimates are relevant. For, in view of the above argument, it is essential to decide whether the dynamics of the order parameter is overdamped at \hat{t} , *i.e.* whether

$$\eta\dot{\varphi}|_{\hat{t}} > \ddot{\varphi}|_{\hat{t}} . \quad (10)$$

This can be evaluated directly from Eq. (2) with the help of the above estimates for \hat{t} and $\hat{\varepsilon}$, and leads to the inequality:

$$(\eta\tau_0)^3 > \frac{\tau_0}{\tau_Q} . \quad (11)$$

Numerical studies have by now confirmed this paradigm. The scalings which we obtained follow theoretical predictions both when the quench is induced by an explicit change of the mass term in Eq. (2) [10–12] and when the temperature of the noise Θ is adjusted, but m set to a constant [13]. Moreover, the switch from the overdamped to the underdamped behavior occurs where expected, and with the consequences consistent with the scaling implied by the paradigm Eqs. (8)–(11) [10–12]. The same reasoning can be of course repeated using other values of critical exponents relevant for other cases [23], which has been already done in some cases [13, 21].

While the scalings accord well with the theoretical predictions, the specific density of defects n is lower than the appropriate inverse power of $\hat{\xi}$

$$n = \frac{1}{(f^2\hat{\xi})^2} , \quad (12)$$

where f is always more than unity, and usually in the range 8–15 [10–13]. We shall return to its estimates later in this paper.

3. Crossover transitions

An interesting case of transitions which does not conform to the second-order universality class occurs when the critical scaling behavior of the healing length and of the relaxation time “tapers off” (*i.e.* is fully analytic) very near to $\varepsilon = 0$. For instance a hypothetical relaxation time and healing length dependences

$$\tau = \frac{\tau_0}{(|\varepsilon| + \Delta)}; \quad \xi = \frac{\xi_0}{\sqrt{|\varepsilon| + \delta}}, \quad (13)$$

illustrate such a crossover transition.

Examples of crossover phenomena are ubiquitous. One of the most interesting cases comes from the study of the electroweak standard model, where, for Higgs masses not yet excluded by experiment, the transition appears to be a crossover [24]. A crossover transition may also occur in the presence of impurities, anisotropies, weak external fields, or finite size scaling, instead of the expected critical behavior of the ideal model. It also substitutes critical behavior when non-perturbative fluctuations exist in the spectrum of the theory which are favored entropically and can destroy long range order. An example of the latter is a $\lambda\phi^4$ theory or a (short-range) Ising model in one spatial dimension.

Thus, τ and ξ in the one-dimensional cases investigated numerically [10, 11] as examples of the second order phase transition are expected to taper off in the immediate vicinity of the critical temperature. Presumably this occurs for very small values of Δ and δ , so that the scaling behavior encountered in the vicinity of $\hat{\varepsilon}$ is not affected. Nevertheless, it is interesting to investigate what does the paradigm predict in the case of such crossover transformations.

We follow the footsteps of the argument outlined in the preceding section, and obtain \hat{t} by solving :

$$\tau(\varepsilon(\hat{t})) = \hat{t}, \quad (14)$$

which now leads to the quadratic equation

$$|\hat{t}|^2 + |\hat{t}|\Delta\tau_Q - \tau_0\tau_Q = 0. \quad (15)$$

Consequently

$$|\hat{t}| = \frac{-\Delta\tau_Q + \tau_Q\sqrt{\Delta^2 + \frac{4\tau_0}{\tau_Q}}}{2}, \quad (16)$$

and

$$|\hat{\varepsilon}| = \frac{-\Delta}{2} + \frac{1}{2}\sqrt{\Delta^2 + \frac{4\tau_0}{\tau_Q}}, \quad (17)$$

where we have picked the physically relevant root of Eq. (15).

We note that in the limit of a ‘real’ second order phase transition ($\Delta \rightarrow 0$) we recover the old result, Eq. (8), providing that the change of notation (τ_0 now used to be $\eta\tau_0^2$ in Eq. (8)) is acknowledged. On the other hand, when the quench is very slow and $\Delta^2 \gg 4\tau_0/\tau_Q$, $\varepsilon \rightarrow \Delta\tau_0/\tau_Q$, which itself is small compared with Δ (and, presumably also δ since $\Delta \sim \delta$ can be expected). Consequently for relatively rapid quenches

$$\hat{\xi} = \frac{\xi_0}{\sqrt{\left(\frac{\tau_0}{\tau_Q}\right)^{1/2} + \delta}}, \quad (18)$$

which approaches Eq. (9) for sufficiently small δ . In the other limit

$$\hat{\xi} = \frac{\xi_0}{\sqrt{\delta}}, \quad (19)$$

and the size of the coherent domains of the order parameter saturates.

We note that the above discussion should be regarded more as an exercise in extending the paradigm rather than as a generically valid theory, applicable to all crossover phase transitions. In particular, in some cases second order transitions may change into crossovers when an external bias which influences the choices of the broken symmetry vacuum is introduced. In such cases the externally imposed (rather than spontaneous) symmetry breaking will favor a particular vacuum and will lead to a suppression of topological defect production [20], [7]).

Moreover, in case of the crossover transitions the influence of the Ginzburg regime may need to be carefully examined as its role in the generation and survival of topological defects is still a subject of dispute.

4. Inhomogeneous transitions

Homogeneous quenches are a convenient idealization and may be a good approximation in some cases. However, in reality, the change of thermodynamic parameters is unlikely to be ideally uniform:

- (1) Experiments carried out in ^3He [15,16], where a small volume of superfluid is re-heated to normal state, and subsequently rapidly cools to the temperature of the surrounding superfluid, are a good example of an inhomogeneous quench: The normal region shrinks from the outside. Yet, topological defects are created, thus suggesting that the phases of distinct domains within the re-heated region are selected independently.

- (2) Another example are relativistic heavy ion collisions where, according to Bjorken scenario [25], a finite volume of quark–gluon plasma can be created. The plasma expands in the direction of collision and cools from the outside in the perpendicular direction. The phase transition in this case can be first or second order (or a smooth crossover) depending on the parameters of the collision.
- (3) Any generic experiment based on pressure and/or temperature quench is to some degree inhomogeneous because of finite velocity of sound and finite heat conductance.

The mass parameter $\varepsilon(t, \vec{r})$, varying in both time and space, must be considered in defect formation. As a consequence, locations entering the broken symmetry phase first could communicate their choice of the new vacuum as the phase ordered region spreads in the wake of the phase transition front. When this process dominates, symmetry breaking in various, even distant, locations is no longer causally independent. The domain where the phase transition occurred first may impose its choice on the rest of the volume, thus suppressing or even halting production of topological defects. This happens if velocity of the critical front is less than certain characteristic velocity.

4.1. Second order transition

The characteristic velocity in an overdamped transition can be estimated as follows: The freeze-out healing length is set at \hat{t} as $\hat{\xi} = \xi_0 (\tau_Q/\tau_0)^{1/4}$. At the same instant the relaxation time is $\hat{\tau} = (\tau_Q\tau_0)^{1/2}$. These two scales can be combined [2] to give a velocity scale

$$\hat{v} = \frac{\hat{\xi}}{\hat{\tau}} = v_0 \left(\frac{\tau_0}{\tau_Q} \right)^{1/4}, \quad (20)$$

where $v_0 = \xi_0/\tau_0$.

The density of defects N as a function of critical front velocity is expected to change qualitatively at \hat{v} . Above \hat{v} the homogeneous estimates should hold. Below \hat{v} the density should be suppressed. Kibble and Volovik [26] suggested that $N \sim v/\hat{v}$ for small $v < \hat{v}$. Dziarmaga, Laguna and Zurek [27] argued that N is exponentially suppressed below \hat{v} . There is qualitative difference between the two proposals. The former option suggests that however one makes a quench one will always get some defects, the latter implies that if one's inhomogeneous quench is sufficiently slow one will get no defects at all. In what follows we will quantify what "sufficiently slow" means.

a. Decay of the False Vacuum. As a simple warm up exercise, let us consider decay of a false symmetric vacuum to a true symmetry broken

ground state in a one-dimensional dissipative φ^4 model

$$\partial_t^2 \varphi + \eta \partial_t \varphi - \partial_x^2 \varphi + \frac{1}{2}(\varphi^3 - \varepsilon \varphi) = 0, \tag{21}$$

where $\varphi(t, x)$ is a real order parameter and ε measures the degree of symmetry breaking *i.e.* $m^2 = -\varepsilon$. Without loosing generality, we look for a solution $\varphi(t, x)$ which interpolates between $\varphi(t, -\infty) = -\sqrt{\varepsilon}$ and $\varphi(t, +\infty) = 0$. Such a solution can not be static. It is a stationary half-kink

$$\varphi(t, x) = -\sqrt{\varepsilon} \left(1 + \exp \left[\frac{\sqrt{\varepsilon} (x - v_t t)}{2 \sqrt{1 - v_t^2}} \right] \right)^{-1} \tag{22}$$

moving with characteristic velocity

$$v_t = \left[1 + \left(\frac{2\eta}{3\sqrt{\varepsilon}} \right)^2 \right]^{-1/2} \underset{\eta \rightarrow \infty}{\approx} \frac{3\sqrt{\varepsilon}}{2\eta}. \tag{23}$$

It is worth noting that the decay velocity v_t increases with ε .

b. Shock Wave. Our shock wave inhomogeneous quench model consists of a sharp “pressure front” propagating with velocity v ; that is,

$$\partial_t^2 \varphi + \eta \partial_t \varphi - \partial_x^2 \varphi + \frac{1}{2}(\varphi^3 - \varepsilon(t, x) \varphi) = \mathcal{O}(t, x), \tag{24}$$

where

$$\varepsilon(t, x) = \text{Sign} \left(t - \frac{x}{v} \right) \tag{25}$$

is the relative temperature and $\mathcal{O}(t, x)$ is a Gaussian white noise of temperature Θ with correlations given by Eq. (3).

There are two qualitatively different regimes:

- (1) $v > v_t$, the phase front propagates faster than the false vacuum can decay. The half-kink (22) lags behind the front (25); a supercooled symmetric phase grows with velocity $v - v_t$. The supercooled phase cannot last for long; it is unstable, and the noise makes it decay into the true vacuum.
- (2) $v < v_t$, the phase front is slow enough for a half-kink to move in step with the front, $\varphi(t, x) = H_v(x - vt)$. The symmetric vacuum decays into one definite non-symmetric vacua. The choice is determined by the boundary condition at $x \rightarrow -\infty$. No topological defects are produced in this regime. The stationary solution $H_v(x - vt)$ is stable against small perturbations [27].

These expectations are borne out by the numerical study of kink formation in [27]. Numerical results are presented in Fig. 1.

c. Linear Front. Let us consider now a system in which the inhomogeneous quench takes place via linear transition

$$\varepsilon(t, x) = \frac{t - \frac{x}{v}}{\tau_Q}. \tag{26}$$

In the absence of noise, the propagating front is followed by a stationary half-kink. This half-kink moves somewhat behind the front. Its location is determined by the place where the threshold velocity (23) is equal to the front velocity, $v_t[\varepsilon(t, x)] = v$. The distance between the front and the half-kink increases as v^3 . This distance gives the size of the supercooled region. When the supercooled region is narrow then it is stable against small perturbations so that no defects are produced. If

$$v > v_t \equiv \left(1 + \frac{\eta^{3/2} \tau_Q^{1/2}}{11.7} \right)^{-1/2} \underset{\eta \rightarrow \infty}{\approx} \frac{3.42}{\eta} \left(\frac{\eta}{\tau_Q} \right)^{1/4} \equiv 4.07 \hat{v}, \tag{27}$$

then the region is broad enough to be unstable [27] and the production of defects is no longer suppressed.

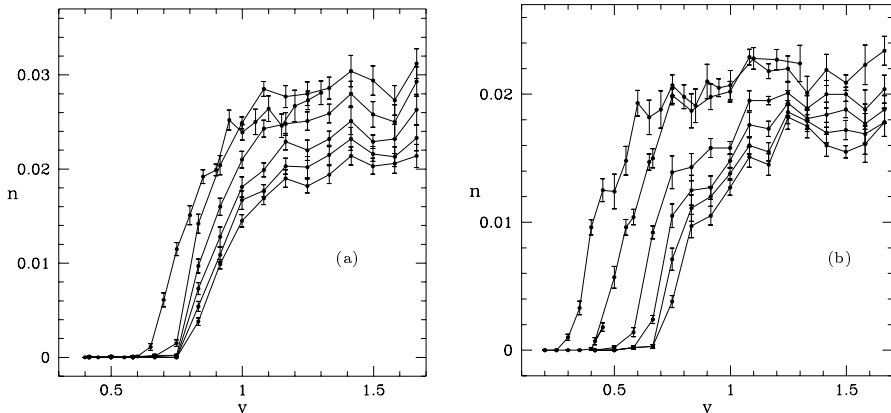


Fig. 1. (a) — density of kinks n as a function of velocity v for the shock wave (25) with $\eta = 1$ (overdamped system). In this overdamped regime, the predicted threshold velocity is $v_t = 0.83$. The plots from top to bottom correspond to $\theta = 10^{-1}, 10^{-2}, 10^{-4}, 10^{-6}, 10^{-8}, 10^{-10}$. At low θ , we get a clear cut-off velocity at $v \approx 0.8$, which is consistent with the prediction. (b) — density of kinks n as a function of velocity v for the linear inhomogeneous quench, Eq. (26), with $\tau_Q = 64$ and $\eta = 1$. The predicted threshold is $v_t = 0.77$. This cut-off is achieved for low θ . The plots from top to bottom correspond to $\theta = 10^{-1}, 10^{-2}, 10^{-4}, 10^{-6}, 10^{-8}, 10^{-10}$.

This prediction is confirmed by the numerical study of linear quenches in Ref. [27], compare Fig. 1. However, the threshold velocity apparently gradually decreases with increasing noise temperature Θ . This decrease of the threshold for kink formation is due to the thermal nucleation of kinks. Quantitative estimates for this effect are given in [28].

4.2. First order transition

We assume the transition is strongly first order and that it goes by bubble nucleation. To be more specific we consider a toy model in 3 dimensions

$$\partial_t \varphi = \nabla^2 \varphi - a\varphi + b\varphi^3 - c\varphi^5 + \mathcal{O}, \quad (28)$$

where φ is real order parameter. The effective potential is of the φ^6 type. Provided that $b^2 > 4ac$, it has symmetric minimum at $\varphi = 0$ and two symmetry broken minima at $\varphi = \pm\varphi_m \equiv \pm\sqrt{(b + \sqrt{b^2 - 4ac})/2c}$. We assume that b, c are constant and that symmetry breaking transition is driven by a decreasing below its critical value $a_c = 3b^2/16c$. At $a = a_c$ all three minima are degenerate.

d. Decay of the False Vacuum. Suppose that $a < a_c$. Let us consider decay of the false symmetric vacuum to the true symmetry broken phase in a one dimensional version of the model Eq. (28). We look for a solution which interpolates between $\varphi = \varphi_m$ for $x \rightarrow -\infty$ and $\varphi = 0$ for $x \rightarrow +\infty$. The solution is a stationary half-kink $H(x - v_t t)$ moving with velocity

$$v_t = \frac{-b + 2\sqrt{b^2 - 4ac}}{\sqrt{3c}} \quad (29)$$

which has an envelope function

$$H(x) = \frac{\varphi_m}{\sqrt{1 + \frac{\exp \alpha x}{2c}}}, \quad (30)$$

where $\alpha = \sqrt{4c/3}\varphi_m^2$. This way the false $\varphi = 0$ vacuum decays into the true $\varphi = \varphi_m$ vacuum in the absence of noise. The decay velocity v_t is zero for $a = a_c$, it increases with increasing supercooling or with decreasing a .

e. Shock Wave. In the shock wave model a sharp front propagates with velocity v

$$a = a_c - \Delta a \text{Sign} \left(t - \frac{x}{v} \right). \quad (31)$$

Similarly as for second order transitions there are two regimes:

- (1) $v > v_t$, the pressure front propagates faster than the false vacuum can decay. The half-kink lags behind the front. The supercooled phase in between them grows linearly with time. The phase is unstable, it decays by bubble nucleation just as for a homogeneous transition. Homogeneous estimates of defect density apply in this case.
- (2) $v < v_t$, the half-kink is faster. It moves in step with the front while its tail penetrating into the symmetric phase. There is no supercooled phase where bubbles could be nucleated. The symmetric phase goes smoothly into one of the symmetry broken phases.

f. Linear Front. Let the inhomogeneous quench proceed by a linear front moving with velocity v

$$a = a_c - \frac{t - \frac{x}{v}}{\tau_Q}. \quad (32)$$

The half-kink follows the critical front staying at a certain distance behind it. The distance D is such that the half-kink velocity v_t , which depends on the local value of a , is equal to the front velocity v , $v_t(a) = v$. With increasing v the half-kink settles at increasing values of local a . Close to the critical front the radius of the critical bubble is infinite and at the same time the nucleation rate is infinitely small. As we go away from the front in the direction of the half-kink the critical radius shrinks. At a certain distance L from the front the energy of the critical bubble becomes comparable to the temperature Θ . At this point bubble nucleation becomes possible. If $L < D$ bubbles can be nucleated in the supercooled region between the front and the half-kink. If $L > D$ then there is no bubble nucleation and no defects can be born in the supercooled area.

Now we estimate the critical velocity such that $L = D$. The half-kink is located at such an a that $v_t(a) = v$. $L = D$ providing that for this a the energy of the critical bubble $E(a)$ is equal to temperature Θ . The critical bubble is a metastable spherically symmetric static solution of Eq. (28) with, say, φ_m vacuum inside and 0 vacuum outside its wall. Its energy can be easily estimated when the width of its wall is negligible as compared to its radius $R_c(a)$. An approximate solution is given by $H[r - R_c(a)]$, where the critical radius is

$$R_c(a) = \frac{\sqrt{12c}}{-b + 2\sqrt{b^2 - 4ac}}. \quad (33)$$

The energy of the critical bubble $E(a)$ has a negative volume contribution, $(4\pi R_c^3/3)V(\varphi_m)$, and a positive surface tension term,

$$(4\pi R_c^2) \int dx [H'(x)]^2.$$

When the solution of $v_t(a) = v$ is put into $E(a)$ and then the equation $E(a) = \Theta$ is solved, one obtains a critical velocity

$$v_{\text{cr}} = \left(\frac{\pi b(3b^2 - 6bc + 16c^2)}{4c^3 \Theta} \right)^{1/3} \quad (34)$$

for $L = D$. For $v > v_{\text{cr}}$ bubbles can nucleate in between the half-kink and the front and thus the necessary condition for topological defects production is satisfied.

The formula for v_{cr} , Eq. (34), is still a crude lower estimate for the critical velocity. In fact it is not sufficient to nucleate some bubbles. Individual bubbles would coalesce with the half-kink without any chance to trap any nontrivial winding number. The bubbles should be nucleated in large numbers or have enough time to grow so that they can mutually coalesce before merging with the half-kink. Still, the argument which leads to v_{cr} demonstrates that there is a threshold velocity for defect formation.

4.3. Higher dimensions

The theory can be generalized to higher dimensions and to a complex order parameter in a straightforward manner. Its major result is that a subthreshold inhomogeneous quench does not produce any variation of the order parameter in the direction normal to the front. This excludes any possibility of production of vortex loops or closed membranes entirely contained in the bulk, as well as of any pointlike defects. Some extended defects can grow into the bulk provided their seeds were created at this edge of the system where the symmetry was broken first. In first approximation such, say, vortices grow into the bulk, following the passing front, while keeping their direction normal to the front. In the end we do not get any chaotic tangle of strings and string loops but parallel “combed” vortices. There are two important perturbations to this “combed” picture:

- (1) Thermal fluctuations make the strings look more random but without backtracking and with string tension tending to smooth the small scale fluctuations. The ends of the strings and antistrings at the critical front are wandering around. Eventually an end of a string and of an antistring may meet so that the strings join into a half-loop with its both ends attached to the initial edge of the system. String tension shrinks the half-loop to the edge where it unwinds.
- (2) A much more efficient factor to remove vortices from the bulk are their mutual interactions. Global parallel string and antistring attract one another so that their ends at the critical front do not seek each other

at random but tend to fuse in a deterministic way. This mechanism makes the number of strings in the bulk decay with increasing distance between the front and the initial edge.

The factors (1) and (2) lead to a picture in which the critical front initially draws some parallel strings and antistrings from the edge, then the strings recombine by joining ends and shrinking back to the edge. In the end only the net surplus of strings (or antistrings) is left in the bulk.

These ideas are supported by experiments:

- (1) Disclinations produced during a quench from disordered to nematic phase in liquid crystals [29]. This is a weakly first order transition. In early attempts to make cosmological experiments in liquid crystals the disclinations were observed to grow approximately combed, join ends and shrink to the initial edge. Later on it was realized that these quenches were not homogeneous enough [30].
- (2) Czochralski method of growing monocrystals, which is widely used to grow silicon monocrystals necessary for microchips. In this method, discovered in the thirties, a surface of liquid material is touched with a monocrystal template. As the template is slowly lifted up it drags a column of crystal out of the container. The top part of the column is cold while its bottom part is at the melting temperature — the transition is inhomogeneous. If the template is lifted slowly enough, then no defects of the crystal lattice are produced which might spoil the monocrystal.

To conclude this section: in an inhomogeneous quench there is a threshold velocity v_t of the critical front. Above the threshold defects are produced like in a homogeneous quench. Below the threshold one gets no defects; instead a clean monocrystal or a “disoriented chiral condensate” is grown with a vacuum which may be uniform over significant distances, but which differs from the true vacuum.

5. Defect formation and the Ginzburg regime

Recently a new ${}^4\text{He}$ experiment [17] was devised, improving on the apparatus used earlier by McClintock *et al.* [31] to implement a superfluid transition in ${}^4\text{He}$ through a sudden pressure quench. The corresponding results are rather surprising. They show no evidence for the formation of topological defects at the anticipated levels, contrary to expectations based both on the old experiment [31], the theory¹ and the ${}^3\text{He}$ data [15,16]. The

¹ Although a factor $f \gtrsim 10$ in the formula for the string density $n \sim 1/(f\xi)^2$ could explain the new results and seems consistent with recent numerical studies [13].

discrepancy with the earlier ^4He quench data is now seen as the evidence of mechanical stirring in the first version of the experiment. Nevertheless to address the discrepancy with ^3He it was suggested [32] that because the Ginzburg regime in ^4He extends over a broad range of temperatures around the λ -line, large scale fluctuations may be able to unwind and alter the configuration of the order parameter (in contrast to ^3He) while the quench proceeds.

The Ginzburg temperature is defined through the loss of ability of the order parameter to hop, through thermal activation, over the potential barrier between broken symmetry vacua. Thus one might worry with Karra and Rivers [32] that when the defect densities are eventually measured, at a much later time, little or no string would have survived unwinding through thermal activation. In this section we investigate this possibility and more generally report a numerical study of the effect of thermal fluctuations on topological defect formation and evolution.

Originally the Ginzburg temperature T_G was suggested to be the time of formation of topological defects [4], since, at lower temperatures, thermal fluctuations would be unable to overcome the potential energy barrier associated with the defect's topological stability.

In reality the situation is more complex. In equilibrium at any given temperature T (including of course temperatures in the Ginzburg regime) a range of string configurations will exist. However, long strings can only exist in equilibrium strictly above T_c [33].

To freeze them out, *i.e.*, to *form* them, energy (associated with the string tension) must be extracted from the system. This necessarily breaks time invariance and will lead to locally preferred nonequilibrium field configurations. Subsequently the system will order over larger and larger spatial scales, leading to mutual string annihilation.

The initial density of defects entering this stage of evolution is computed by the theory of Section 2. This density is set at an effective temperature $-\hat{\varepsilon}$, which in ^4He is well within the estimates for the width of the Ginzburg regime. By contrast, in ^3He the Ginzburg temperature is small compared to the typical $\hat{\varepsilon}$. What happens to the initial densities of string when the system is exposed to temperatures in the Ginzburg regime for an extended amount of time?

In order to investigate this issue we need a quantitative definition of T_G . In tune with the arguments given above consider a volume of characteristic size $\xi(T)$, the correlation length, and a theory with two energetically degenerate minima of an effective potential $V(\phi)$, separated by a potential barrier ΔV . The rate for the field to change coherently from one minimum to the other per unit volume due to thermal activation is $\exp[-\Delta V/k_B T]$. For an effective potential of the form (obtained, *e.g.* perturbatively at 1-loop)

$$V(\phi) = -\frac{1}{2}m^2(T)\phi^2 + \lambda\phi^4, \quad (35)$$

$\Delta V = \frac{m(T)^4}{4\lambda}$. For a volume ξ^3 , we define T_G such that the probability of overcoming the potential barrier is of order unity:

$$T_G : \frac{\Delta V(T_G)}{T_G} \xi^3(T_G) = 1 \quad \Leftrightarrow \quad \frac{\lambda T_G}{m(T_G)} = \frac{1}{4}. \quad (36)$$

This definition however has some caveats, for instance, an effective potential of the form Eq. (35) is only valid for the mean field and not on smaller scales. A more careful accounting of scales leads to different results [34], which show an enhancement of the hopping probability. Thus, the factor of 1/4 in Eq. (36) should not be taken at face value.

A more rigorous definition arises from the range of temperatures below T_c for which fluctuations are large and consequently where perturbative finite temperature field theory fails to be useful. In order to set up a perturbative scheme at finite temperature from an initial 3 + 1 dimensional quantum field theory one implements dimensional reduction which is valid provided the temperature is high compared to all mass scales. As a consequence the coupling of the dimensionally reduced 3D field theory becomes dimensionful, *i.e.* $\lambda \rightarrow \lambda T = \lambda_3$. In order to proceed one has to identify an appropriate dimensionless coupling. This is done by taking $\lambda T/m(T)$. The Ginzburg regime is entered when this 3D effective coupling becomes strong, in the vicinity of the critical point, namely

$$T_G : \frac{\lambda T_G}{m(T_G)} = 1. \quad (37)$$

To compute T_G one needs the scaling of $m(T)$ in the critical domain. We write $m^2(T) = m_0^2 \varepsilon^\nu$, with ε being the reduced temperature $\varepsilon = |\frac{T-T_c}{T_c}|$.

Thus $\varepsilon_G = -0.18$ for $\nu = 0.5$. This mean-field estimate produces an upper bound in T for T_G (and lower bound for $\beta = 1/T$). For realistic 3D exponents, $\nu = 0.67$, we obtain $\varepsilon_G = -0.25$. The first criterion, based on the hopping of a correlation sized volume, results in higher values of T_G . This brings about a relatively large uncertainty in the value of T_G , which is 18–25% below T_c .

5.1. Strings survive the Ginzburg regime

In order to investigate the role of the Ginzburg temperature in the *dynamics* of defect formation we deliberately expose the system to a heat bath at temperature ε_i , within the Ginzburg regime and below. We repeat this procedure for a range of time intervals Δt , after which the bath temperature is taken to zero. This set of temperature trajectories is shown in Fig. 2. We are attempting to emulate the worst case scenario of an experimental quench

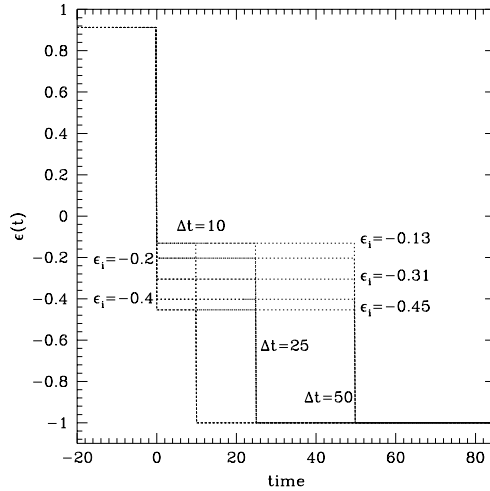


Fig. 2. Temperature trajectories for testing the effect of exposure to the Ginzburg regime on string densities. The system is first thermalized at a high temperature and then placed in contact with a heat bath at an intermediate temperature ε_i below T_c , for a time interval Δt .

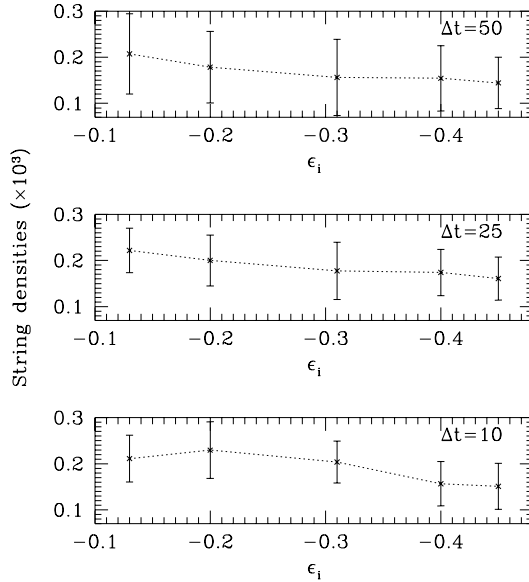


Fig. 3. The string density measured at a later time $t \gg \Delta t$ vs intermediate temperature ε_i . From top to bottom the three plots correspond to $\Delta t = 10, 20, 50$, during which the system remained in contact with a heat bath at T_i . There is no visible role played by intermediate temperatures within the Ginzburg regime.

where the temperature or pressure are dropped monotonically but where the system makes a long stopover within the Ginzburg regime.

We would expect that, if the Ginzburg regime indeed produced enhanced decay of strings, then the string densities measured at later times should be smaller the longer the time the system spent within the range $T_c \geq T \geq T_G$.

We have measured the final string densities at a time $t \gg \Delta t$. Our results for the final string densities as a function of intermediate temperature ε_i and Δt are summarized in figure 3. There is no apparent effect of the Ginzburg regime in reducing string densities at formation.

If any trend is visible from figure 3 it is the opposite, namely that the lower ε_i , the less string is measured at later times. This is consistent with the relaxation of the string network, resulting in vortex annihilation controlled by the string tension (which is smaller near T_c) and with results the thermodynamics of vortex strings [33].

5.2. Memory of the order parameter configuration near T_c

An independent test on the possible role of thermal fluctuations in affecting string densities consists in reheating a quenched system to a temperature around T_c (both below and above it) and cooling it again. This process tests the memory of the order parameter as well as that of other related quantities (see also [12]), such as defects. These temperature ($\varepsilon(t)$) trajectories are illustrated in Fig. 4(a).

We are particularly interested in investigating under what circumstances thermal fluctuations can affect the large scale configuration of the order parameter.

We define the unequal-time correlation function

$$\langle \varphi(x, t_{\text{rh}}) \varphi(x, t + t_{\text{rh}}) \rangle = N \sum_{j=1}^2 \sum_i \varphi_j(x_i, t_{\text{rh}}) \varphi_j(x_i, t + t_{\text{rh}}), \quad (38)$$

where N is an irrelevant normalization factor. Note that the correlation function $\langle \varphi(x, t_{\text{rh}}) \varphi(x, t + t_{\text{rh}}) \rangle$ cannot be complex as we have summed over the field's components. This correlator has several interesting properties. For short times it displays a characteristic time, which describes the decay of correlations over very small spatial scales. This is the initial transient in Fig. 4(b). For later times the residual correlation comes from the motion of the order parameter (the field volume average). This average can be either positive or negative but, if thermal, will converge to zero at and above T_c .

Now, we are interested in determining whether the final field configuration over large spatial scales is correlated to the configuration prior to reheating. Fig. 4 shows that only if one crosses T_c , by more than $+\hat{\varepsilon}$, is the

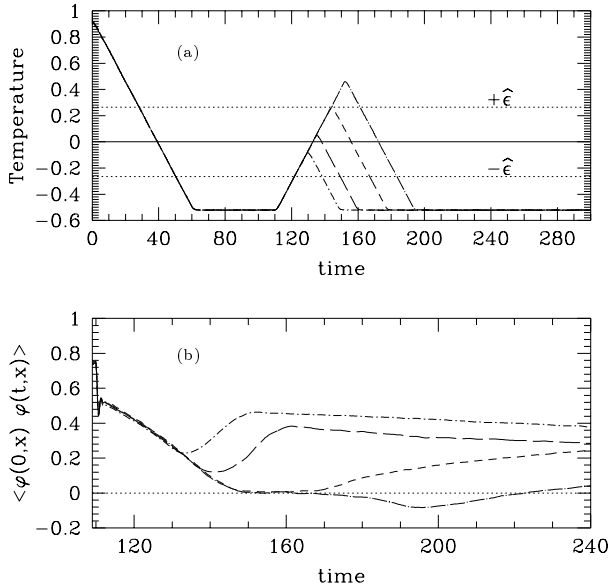


Fig. 4. (a) — dependence of the bath temperature ϵ in time. After being quenched in temperature ($\tau_Q = 80$) the system is reheated at the same τ rate to a temperature $\epsilon_f = 0.469, 0.256, 0.061, -0.068$ (top to bottom) ‘and cooled again. (b) — the correlation function between the field at the time just before reheating and at later times, $\langle \varphi_i(t_{rh}, x) \varphi_i(t + t_{rh}, x) \rangle$ is plotted. There is a universal short time transient for the decorrelation of the field over small scales while the long time tails of the correlation function describe change over the mean fields. All four trajectories cross the Ginzburg regime, but only those reaching or crossing $+\hat{\epsilon}$ display a significant memory loss.

memory of the initial quenched configuration erased (see in particular the two trajectories reaching higher temperatures in comparison to the others). For these trajectories the field correlations reach zero and after reheating evolve to a value manifestly different from that prior to reheating.

For trajectories within the Ginzburg regime, that do not cross T_c , the change in the configuration of the order parameter as measured by Eq. (38) is small. In particular the field configuration existing before reheating is approximately recovered as the fields are cooled. The same is true for the string densities, including those of long strings.

Thus we are led to conclude (see also [33]) that even prolonged exposure of a quenched field configuration to the Ginzburg regime has little consequences in changing the order parameter configurations emerging at $-\hat{\epsilon}$, and associated string densities. In addition we have shown that to truly destroy a quenched field configuration existing below $-\hat{\epsilon}$, one has to expose the sys-

tem to temperatures well above T_c . In particular for any particular quench trajectory, a temperature of $T \sim T_c + \hat{\varepsilon}$, must be reached and maintained for a time $\sim \hat{t}$ in order to erase memory of the initial configuration.

These results fully support the theory of Section 2 for the critical dynamics of second order transitions and all known thermodynamic results for vortex strings in $O(N)$ theories. Thus we expect the results of this section to carry over from our models to the Lancaster ${}^4\text{He}$ experiments. The results of Ref. [17] in these experiments cannot therefore be attributed to the effects of Ginzburg regime in ${}^4\text{He}$.

In the next section we offer an alternative explanation.

6. What is being observed in the ${}^3\text{He}$ and ${}^4\text{He}$ experiments

The several experiments in Helium, and more recently in superconductors, testing the theory of defect formation rely on substantially different processes to induce the phase transition and measure defects.

In this section we analyze, in the light of our own theoretical results, how experimental procedures can lead to the detection of substantially different defect densities.

Two particular factors play a decisive role in the value of the topological defect density measured — the time and procedure of measurement after the quench and the initial/final state of the system.

6.1. The Lancaster experiments in ${}^4\text{He}$

In the Lancaster experiments in ${}^4\text{He}$ the defect density is measured through the attenuation of a second sound signal (a heat pulse). This probe can only detect densities above a certain threshold (if the theory of Section 2 is used $f \leq 10$ would be required, which is at odds with the results of the numerical studies [10, 12] and especially [13]). Moreover, the density at formation has to be extrapolated from the data obtained at relatively late times — the signal is noisy shortly after the quench [17].

After being formed by the critical dynamics of the phase transition vortex strings decay away, as the system orders and cools. This decay has been modeled by Vinen's Equation

$$\dot{n} = -\gamma n^2, \quad (39)$$

where n is the length of string per unit volume, *i.e.* the string length density, $\gamma > 0$. This model has been observed in the same experiment to describe very well the decay of vorticity induced initially through a fluid flow.

Vorticity created thermally is potentially different from that formed under an external flow. We know from several theoretical and numerical in-

indications that a thermal distribution of vortices close to the transition is comprised of both long strings and small loops, see Fig. 5.

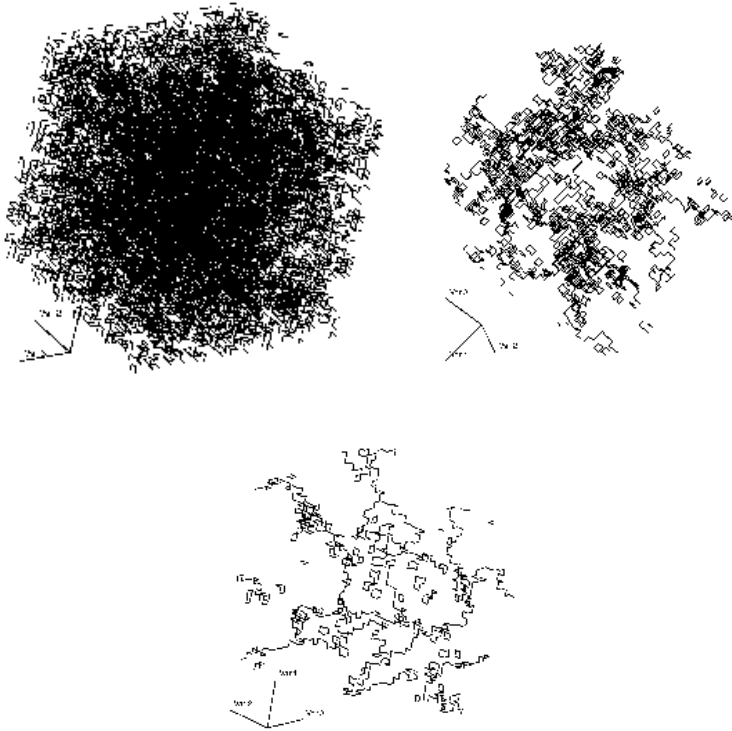


Fig. 5. The decay of vorticity under a quench. Initially the defect network includes both long strings and small loops. At late times the network coarsens and only long strings remain, see also Fig. 6.

These two populations decay very differently in the wake of the quench. Without any mechanism for stabilization the loops tend to disappear in a fast transient. In contrast the long strings loose some of their small scale structure but survive, and will ultimately set the decay pattern described by the Vinen equation.

It is the surviving long strings — eventually measured — that will provide the experimental signal in the ^4He experiments. This is shown in Figs. 5 and 6. As the system is quenched from higher temperatures or pressures, an initial string network comprised of strings of all lengths looses its loops and settles to a much slower decay trend dominated by long strings.

The crucial question then is whether enough long string would persist at the time of measurement to yield a positive signal.

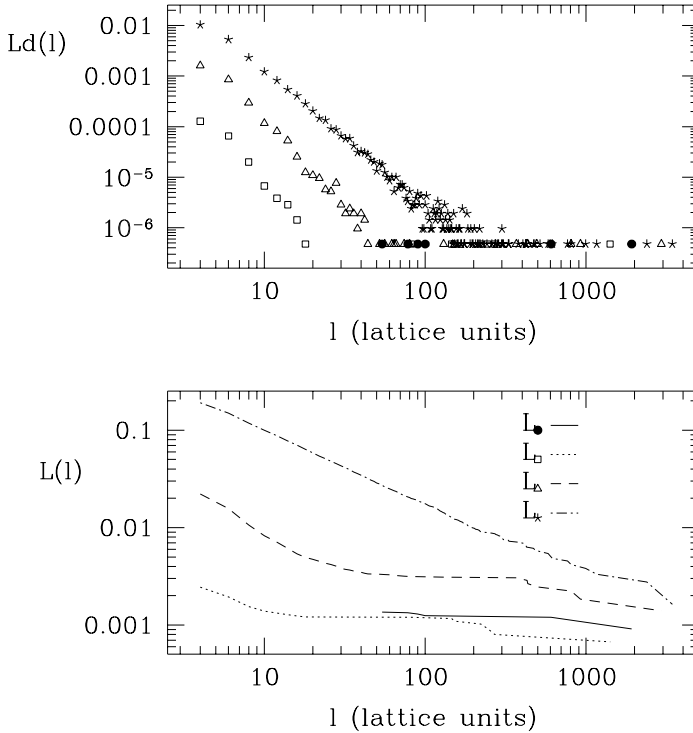


Fig. 6. String length l distributions $L_d(l)$, taken between $+\hat{t}$ and the “time of formation” ($\langle|\phi|\rangle = 0.95$), for $\tau_Q = 64$. Data sets denoted by ($\star, \Delta, \square, \bullet$) correspond to increasingly later times. Lines show the integral distributions, e.g. $L_{\bullet}(l) = \sum_l^{\infty} l' L_{\bullet}(l') dl'$. It is clear that at late times only long strings survive.

We have performed a very similar procedure in a numerical “experiment” [13]. We observed that at long times string densities could be measured that agreed extremely well with all features of the theory. Our definition of *long* times was intimately connected to the completion of the phase transition expressed in the expectation values of the order parameter $\langle|\phi|\rangle \simeq 0.9\text{--}0.975$. The effective f measured then was in the range $f = 11\text{--}16$. All our indications are that the Lancaster ${}^4\text{He}$ experiment performs its measurements much later (up to 2 orders of magnitude) than we do, thus leading to even smaller string densities. Such string densities could evade detection under the second sound experimental probe, which may lead to the negative result [17].

The other possibility is that the annihilation of a network of vortices arising from a rapid quench may proceed at a rate different than for the network produced by turbulent flow. Clearly, in case of turbulent flow there may be

correlation between the orientation of nearby vortices. By contrast, vortices created by quench are anticorrelated (see, *e.g.*, discussion in Section 4 of Ref. [21]). It seems plausible that annihilation of vortices would be faster in that case. In order to measure a positive signal in these circumstances the measurements would have to be made sooner, after a much faster quench, or with a higher sensitivity.

6.2. Experiments in ${}^3\text{He}$

In contrast to the experiments in ${}^4\text{He}$ described above which appear sensitive to the “infinite” string, experiments in ${}^3\text{He}$ have pursued two independent strategies both of which allow one to stabilize and detect defect loops of various sizes: either vorticity is stabilized and amplified by the flow and then measured directly using nuclear magnetic resonance (the Helsinki experiment) or it is inferred from a certain amount of missing energy (the Grenoble and Lancaster ${}^3\text{He}$ experiments). Of these two procedures the first is more direct — vorticity formed during the quench is forced to migrate to the center of the container, through the existence of a subcritical rotation velocity, where it is detected. This permits loops of string of length larger than a known threshold to survive decay and results naturally in a higher density, *i.e.* the defect density is measured effectively very shortly after the transition takes place and need not be limited the “infinitely long string”. As a consequence, much smaller values of f and larger string densities are measured than in the ${}^4\text{He}$ experimental setting.

Both remaining ${}^3\text{He}$ experiments end at a region of the phase diagram far from the transition — ${}^3\text{He}$ being very much colder than in the Helsinki experiment. A lower effective temperature results in the effective absence of damping mechanisms which in turn leads to the preservation of even small vortex loops. Dissipation mechanisms rely on the presence of quasiparticles. Thus, when the medium is very cold, energy dissipation will slow exponentially and vortices can be stabilized by a coherent flow resulting from their motion through the superfluid. We expect therefore the string population in all ${}^3\text{He}$ experiments to be mostly in the form of relatively small loops. In Helsinki, the largest loops are stabilized by the slow rotation of the whole system, and their density can be extrapolated to the smaller loops, leading to the total consistent with the Grenoble and Lancaster experiments, where — one may guess — all of the loops survive for a long time in the absence of dissipation.

The lifetime of these loops is thus expected to be much longer than that of thermal loops formed at a quench through the λ -line in ${}^4\text{He}$. As a result the long time decay of vorticity may also be very different in these two cases as the former corresponds to an ensemble of moving loops, at relative distances

much larger than their typical radius, but the latter contains strings of all sizes, where the mean distance between strings is comparable to their length.

This conjectured picture, supported in part by numerical studies, leads to the conclusion that both experimental settings in ^3He should lead to a positive result, compatible with a relatively small value of f relevant for all loops (we get $f \simeq 4$, when $n \sim 1/(\hat{\xi}f)^2$ is used to fit early data in Fig. 6), whereas in ^4He the smallness of the signal at the time of first measurement makes the detection more difficult and at present below the sensitivity threshold.

7. Discussion

The mechanism we described early on in this paper is based on the analysis of the behavior of the order parameter φ . The order parameter is clearly a phenomenological entity and the equations that govern its evolution are approximate and in many cases postulated rather than derived. On the other hand the underlying physics is usually very specific. It may, for instance, involve atoms of some particular isotope such as ^4He . Thus, in principle, one could formulate an exact microscopic theory of particular second order phase transformations. However, in all of the experimentally accessible cases discussed above such a fundamental theory is simply too complicated to lead to useful conclusions. The superfluid transition in ^4He is a good example: Strong interactions in ^4He make it impossible to proceed rigorously all the way starting at the microscopic level. Analysis of related issues in the field theoretic context is also difficult [35]. Recently however a new system has become experimentally accessible: Atomic Bose–Einstein Condensates (BEC’s) undergo the second-order phase transition at much lower densities. Natural approximation schemes can be therefore suggested, and the exact microscopic theory can be studied in greater detail than for the “old” superfluids.

We shall not attempt to review the theoretical or experimental situation in BEC’s. Good reviews already exist (see *e.g.* [36]). Our aim is simply to point out that questions concerning the formation of topological defects can be posed and analyzed within a much more fundamental formalism, which is explicitly quantum. The approximations start from the Schrödinger, equation and lead in a controlled manner to master equations for the density operator of the condensing system. Further approximations result in a quantum kinetic theory. Preliminary analysis of these issues [37] allows one to recover the key scaling relations and the key predictions we have described in Section 2. Indeed, time dependent Landau–Ginzburg theory follows as an approximation to some of the terms which one obtains from the microscopic treatments. On the other hand, the microscopic theory contains additional

terms, which alter predictions concerning the formation of topological defects. Limited studies [37] indicate that the predicted densities of the vortex lines or of the winding numbers would be smaller than those based on the scalings of the order parameter (see Section 2 of this paper). Moreover, corrections seem to be more significant as the ratio τ_0/τ_Q decreases.

The possibility of experimental studies of defect formation in BEC quenches nevertheless exists and may lead to exciting insights into the problem.

Superconductors may be the other useful testing ground. Indeed, two experiments have been already reported [18], with the claim of conflicting results, which seemed to depend on the geometry. Rapid cooling produced no detectable signal in a high-temperature film, although it is far from clear whether any was expected. The original claim that the effect was ruled out at the “ $\sim 10^3$ level” was based on an overly optimistic prediction, which did not recognize that the total flux expected to arise in the experimentally studied geometry scales as $n^{1/4}$, *i.e.* only with the *fourth root* of the total number of defects (rather than with the square root; see Section 4 of Ref. [21] for discussion).

The revised prediction is close to the claimed sensitivity of the experiment, and given the uncertainties in the critical exponents of the high-temperature superconductor, as well as the possibility of imperfect trapping of the defects, *etc.* it is unfortunately impossible to extract useful constraints from the existing negative experiment.

The experiment carried out by the same group, in the loop geometry has, on the other hand, yielded positive results. This experiment also operates near the edge of detectability. It detects the flux induced by a loop which is artificially broken into a large number N of superconducting sections, which are then rapidly reconnected. The predicted flux should have a Gaussian distribution with a random direction and intensity corresponding to $\sigma \sim \sqrt{N}$ flux quanta [21], such signals appear to have been indeed found [18].

The available experimental results can be therefore described as confusing. In liquid crystals the results seem to be the perhaps least ambiguous, but they concern a (weakly) first order transition. In superfluids, ^3He is still the strongest case for the mechanism, especially since the results between all the experiments (carried out in quite different parameter regimes, and using very different techniques) are consistent. On the other hand the relevance of the Helsinki experiment for the cosmological scenario has been recently questioned by numerical experiments [38] which indicate that the vorticity generated in such settings may be induced by the flow imposed in the Helsinki experiment to facilitate the process of their detection. These simulations were carried out under a very idealized set of assumptions (which included very small fluctuations and axial symmetry) and conclusions of

Ref. [38] appear to be inconsistent with the experiment [39], but much more remains to be done to clarify this issue. Indeed, a fully 3-D study with large fluctuations is under way [40]. Further experimental and numerical studies to investigate the role of rotation in stabilizing vortex loops and to explore the implications for the A–B phase transition, *etc.*, are nevertheless essential.

The existing ^4He data are clearly disappointing, but not at odds with a more conservative theoretical estimate. Moreover as we have argued above there may be a way to reconcile estimates of vortex line density obtained from ^3He and ^4He experiments, even without any special appeal to the Ginzburg regime [32] or to quantum kinetic theory.

Finally the first experimental reconnaissance into quenches in superconductors is preliminary in its nature and ambiguous in its results.

In the meantime, numerical studies have confirmed and refined the basic indications of the theory of order parameter dynamics.

One may be therefore justified in the expectation of an exciting but uncertain future. A lot is at stake, including the understanding of the phase transition dynamics, nature of the order parameter and other collective observables of quantum many body systems and perhaps even the relation between the quantum and the classical.

REFERENCES

- [1] W.H. Zurek, Experimental Cosmology: Strings in Superfluid Helium, Los Alamos preprint LA-UR-84-3818.
- [2] W.H. Zurek, *Nature* **317**, 505 (1985).
- [3] W.H. Zurek, *Acta Phys. Pol.* **B24**, 1301 (1993).
- [4] T.W.B. Kibble, *J. Phys. A* **9**, 1387 (1976).
- [5] T.W.B. Kibble, *Phys. Rep.* **67**, 183 (1980).
- [6] A.J. Gill, hep-ph/9706327.
- [7] J. Dziarmaga, *Phys. Rev. Lett.* **81**, 5485 (1998); J. Dziarmaga, M. Sadzikowski, *Phys. Rev. Lett.* **82**, 4192 (1999).
- [8] G. Volovik, *Czech J. Phys.* **46**, 3048 (1996).
- [9] Y.M. Bunkov, O.D. Timofeevskaya, *Phys. Rev. Lett.* **80**, 1308 (1998).
- [10] P. Laguna, W.H. Zurek, *Phys. Rev. Lett.* **78**, 2519 (1997).
- [11] P. Laguna, W.H. Zurek, *Phys. Rev.* **D58**, 5021 (1998).
- [12] A. Yates, W.H. Zurek, *Phys. Rev. Lett.* **80**, 5477 (1998).
- [13] N.D. Antunes, L.M.A. Bettencourt, W.H. Zurek, *Phys. Rev. Lett.* **82**, 2824 (1999).

- [14] G.J. Stephens, E.A. Calzetta, B.L. Hu, S.A. Ramsey, *Phys. Rev.* **D59**, 045009 (1999).
- [15] C. Bäuerle *et al.*, *Nature* **382**, 332 (1996).
- [16] V.M.H. Ruutu *et al.*, *Nature* **382**, 334 (1996); V.M.H. Ruutu *et al.* *Phys. Rev. Lett.* **80**, 1465 (1998).
- [17] M.E. Dodd *et al.*, *Phys. Rev. Lett.*, **81**, 3703 (1998).
- [18] R. Carmi, E. Polturak, *Phys. Rev.* **B60**, 7595 (1999); R. Carmi, E. Polturak, G. Koren, *Phys. Rev. Lett.* **84**, 4966 (2000).
- [19] G.D. Lythe, *Anales de Fisica* **4**, 55 (1998).
- [20] J. Dziarmaga, *Phys. Rev. Lett.* **81**, 1551 (1998).
- [21] W.H. Zurek, *Phys. Rep.* **276**, 177 (1996).
- [22] V.B. Eltsov, M. Krusius, G.E. Volovik, cond-mat/9809125.
- [23] P.C. Hohenberg, B.L. Halperin, *Rev. Mod. Phys.* **43**, 435 (1977).
- [24] K. Kajantie, M. Laine, K. Rummukainen, M. Shaposhnikov, *Phys. Rev. Lett.* **77**, 2887 (1996).
- [25] J.D. Bjorken, *Phys. Rev.* **D 27**, 140 (1983).
- [26] T.W.B. Kibble, G.E. Volovik, *Zh. Eksp. Teor. Fiz.* **65**, 96 (1997).
- [27] J. Dziarmaga, P. Laguna, W.H. Zurek, *Phys. Rev. Lett.* **82**, 4749 (1999).
- [28] N.B. Kopnin, E.V. Thuneberg, *Phys. Rev. Lett.* **83**, 116 (1999).
- [29] I. Chuang, R. Dür rer, N. Turok, B. Yurke, *Science* **251**, 1336 (1991); M.J. Bowick, L. Chander, E.A. Schiff, A.M. Srivastava, *Science* **263**, 943 (1994).
- [30] B. Yurke, private communication.
- [31] P.C. Hendry *et al.*, *Nature* **368**, 315 (1994).
- [32] G. Karra, R.J. Rivers, *Phys. Rev. Lett.* **81**, 3707 (1998).
- [33] N.D. Antunes, L.M.A. Bettencourt, M. Hindmarsh, *Phys. Rev. Lett.* **80**, 908 (1998); N.D. Antunes, L.M.A. Bettencourt, *Phys. Rev. Lett.* **81**, 3083 (1998); L.M.A. Bettencourt, N.D. Antunes, W.H. Zurek, *Phys. Rev.* **D62**, 5005 (2000).
- [34] L.M.A. Bettencourt, *Phys. Lett.* **B356**, 297 (1995).
- [35] D. Boyanovsky, H. de Vega, R. Holman, Non-Equilibrium Phase Transitions in Condensed Matter and Cosmology: Spinodal Decomposition, Condensates and Defects, in Ref. [41].
- [36] W. Ketterle, D.S. Durfee, D.M. Stamper-Kurn, cond-mat/9904034.
- [37] J.R. Anglin, W.H. Zurek, *Phys. Rev. Lett.* **83**, 1707 (1999).
- [38] I.S. Aranson, N.B. Kopnin, V.M. Vinokur, *Phys. Rev. Lett.* **83**, 2600 (1999).
- [39] G.E. Volovik, *Physica* **B280**, 122 (2000).
- [40] L.M.A. Bettencourt, W.H. Zurek, in preparation.
- [41] Y.M. Bunkov, H. Godfrin, *Topological Defects and the Nonequilibrium Dynamics of Symmetry Breaking Phase Transitions*, Kluwer, Dordrecht 2000.